NeuroImage 317 (2025) 121320

Contents lists available at ScienceDirect

NeuroImage

journal homepage: www.elsevier.com/locate/ynimg

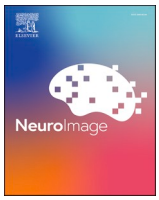

Neurovascular coupling of inhibitory control in late-onset depression: a simultaneous EEG-fMRI study

Elena Bondi [a,b], Alessandro Pigoni [c], Adele Ferro [c], Maria Pia Marra [c], Guido Nosari [c], Giandomenico Schiena [c], Fabio M. Triulzi [d], Anna M. Bianchi [b,e], Paolo Brambilla [a,c,1,*], Eleonora Maggioni [b,c,1]

[a] Department of Pathophysiology and Transplantation, Università degli Studi di Milano, Milan, 20122, Italy
[b] Department of Electronics, Information and Bioengineering, Politecnico di Milano, Milan, 20133, Italy
[c] Department of Neurosciences and Mental Health, Fondazione IRCCS Ca' Granda Ospedale Maggiore Policlinico, Milan, 20122, Italy
[d] Neuroradiology Unit, Fondazione IRCCS Ca' Granda Ospedale Maggiore Policlinico, Milan, 20122, Italy
[e] Fondazione IRCCS Ca' Granda Ospedale Maggiore Policlinico, Milan, 20122, Italy

ARTICLE INFO

Keywords:
Simultaneous EEG-fMRI
MDD
Inhibitory control
N2
P3
Go/No-Go

ABSTRACT

Depression is a leading cause of disability that exerts an impact on neurocognitive functions. Individuals with major depressive disorder (MDD) have shown alterations of processes underlying response inhibition, which is the cognitive process that permits the suppression of habitual or natural behavioural responses to stimuli to select a more appropriate response that is coherent with the goal; these alterations have been correlated with cognitive deficits, especially in older adults. Electrophysiological (EEG) and functional magnetic resonance imaging (fMRI) studies have investigated the neuronal and hemodynamic process underlying inhibition through tasks measuring the ability to suppress a dominant response when non-target stimuli are shown and reported differences between healthy controls (HCs) and MDD subjects. However, these were unimodal studies that provided an incomplete picture of the phenomenon, due to the single technique sensitivity and limited by the characteristics of each technique itself.

In this study, we performed an EEG-driven fMRI analysis to explore the different hemodynamic correlates of specific event-related potentials (ERPs) of inhibitory control in late-onset MDD during a visuomotor Go/No-Go task. The dataset was composed of 18 older adult HCs and 18 late-onset MDD patients.

Behavioral analysis showed higher response time to target stimuli in inhibitory blocks and lower percentage of correct answers for target stimuli in MDD compared to HCs. ERP analysis revealed the inhibitory effect for both N2 and P3 in both groups. Moreover, EEG-driven fMRI analysis showed alterations in the MDD group in the superior temporal gyrus and cerebellar areas for N2 correlates, whereas in the supramarginal, left rolandic, and Heschl's areas for P3 correlates.

The study showed the potentiality of the EEG-fMRI integration for investigating complex cognitive processes. Specifically, the EEG-driven fMRI analyses showed different correlates for separate cognitive processing steps, N2 and P3, highlighting differences between MDD and HC.

1. Introduction

Inhibitory control is the ability to override habitual, dominant, or behavioral responses to stimuli and to choose a more suitable response consistent with the goal. Response inhibition is a central component of executive functions (Norman and Shallice, 1986), but can be separated

Abbreviations: MDD, major depressive disorder; HC, healthy controls; HDRS, Hamilton depression rating scale; SSRI, selective serotonin reuptake inhibitors; SNRI, serotonin and norepinephrine reuptake inhibitors; RBANS, repeatable battery for assessment of neuropsychological status; AAL, automated anatomical labeling atlas; T, T-statistics; p, p-value; k, cluster-based thresholding; x y z, MNI coordinates expressed in mm; L, left; R, right.

* Corresponding author at: Department of Neurosciences and Mental Health, Fondazione IRCCS Ca' Granda Ospedale Maggiore Policlinico, Via Sforza 35, 20122 Milan, Italy.
E-mail address: paolo.brambilla@policlinico.mi.it (P. Brambilla).

[1] These authors contributed equally to this work.

https://doi.org/10.1016/j.neuroimage.2025.121320
Received 26 August 2024; Received in revised form 6 June 2025; Accepted 10 June 2025
Available online 11 June 2025

at a cognitive level from other major executive processes (Miyake et al., 2000). Therefore, inhibition created a great interest in the neuroscience field, leading to the investigation of the process in health (Bokura et al., 2001; Benikos et al., 2013) and psychiatric disorders (Rentrop et al., 2007; Wessa et al., 2007; Ruchsow et al., 2008; Tikàsz et al., 2018). The study of inhibitory control in major depressive disorder (MDD) is of particular interest (Murphy et al., 1999; Kaiser et al., 2003; Zhang et al., 2007; Ruchsow et al., 2008; Quinn et al., 2012; Han et al., 2020), given its association with cognitive control deficits, such as rumination, difficulty in concentration, deterioration of externally oriented attention, selective attention, and self-focused thinking (Knyazev et al., 2018). This is even more relevant in late-life MDD, a pathology that has been associated with executive dysfunctions (Bessette et al., 2020). In this context, the pathology has been associated with fronto-striatal abnormalities that might lead to the executive control alterations (Katz et al., 2010; Zhang et al., 2007).

Literature studies of inhibitory control commonly relied on the Go/No-Go task, which is a simple paradigm where subjects are asked to respond to "Go" stimuli and withhold it to "No-Go" stimuli. Unlike the stop-signal task, the Go/No-Go task inhibits the motor response before initiating the response (Swick et al., 2011), leading to motor preparation for both stimuli (Zhang et al., 2007). Two meta-analyses (Swick et al., 2011; Criaud and Boulinguez, 2013) investigated the functional magnetic resonance imaging (fMRI) correlates of the Go/No-Go task in healthy controls (HC). Swick et al. (2011) reported activations in the anterior insula, left superior frontal gyrus, and strong right lateralization in the middle frontal gyrus and inferior parietal gyrus (IPG), showing the importance of anterior insula, supplementary motor area (SMA), and pre-SMA for successful response inhibition. However, according to Criaud et al. (2013) these regions are not directly related to the inhibition process and could reflect the engagement of different cognitive processes. In their work, they analyzed thirty "Go/No-Go" fMRI studies on healthy subjects suggesting that both "Go" and "No-Go" stimuli induce inhibition because of the uncertainty of the next event, leading to difficulty in finding the inhibition circuits when "No-Go" > "Go" contrast is investigated.

Besides neuroimaging studies, inhibitory control has been largely investigated using electrophysiological (EEG) measures, such as event-related potentials (ERP). The high temporal resolution of the EEG allows us to detect changes in cortical activity in the order of a few milliseconds in response to specific "Go/No-Go" stimuli (Eimer, 1993; Falkenstein et al., 1999). ERP can be described as a series of positive and negative deflections that can be characterized by their amplitude and latency. The inhibitory process is mainly identified by two components in the frontal region: the N2, a negative deflection around 200 ms after the stimulus, and the P3, a positive deflection occurring about 300 ms post stimulus. Falkenstein et al. (1999) reported the "Go/No-Go" N2 effect as a more negative frontal deflection of the N2 peak in the "No-Go" condition that characterizes the response inhibition process. EEG source analyses located N2 peak in the anterior cingulate cortex (ACC) (Bokura et al., 2001) and inferior frontal gyrus (Huster et al., 2010; Enriquez-Geppert et al., 2010), and is thought to reflect the first stage of inhibition and to be related to conflict monitoring (Falkenstein et al., 1999; Nieuwenhuis et al., 2003; Donkers and Van Boxtel, 2004). "No-Go" P3 was found in the frontocentral regions with a higher amplitude with respect to "Go" P3 (Bokura et al., 2001). In visual Go/No-Go task, P3 has been associated with the identification, evaluation, or categorization of the stimuli and context (Polich, 2007) and has been suggested to be related to the second stage of inhibition (Garavan et al., 1999), closely related to the inhibition of the motor response in the premotor cortex. Source localization analysis found P3 in more posterior regions with respect to N2, showing both anatomical and functional differences (Huster et al., 2010). Few "Go/No-Go" studies investigated the inhibitory control process in MDD patients using EEG. An auditory "Go/No-Go" ERP study showed a reduction of the fronto-temporal positivity of the inverted N2 in MDD (Kaiser et al., 2003). Instead, inconsistent results were found in visual "Go/No-Go" studies, with Zhang et al. (2007) who found larger "No-Go" N2 and smaller "No-Go" P3 in the depressed group, whereas Katz et al. (2010) found a strongly reduced No-Go-N2 enhancement in MDD. Regarding neuroimaging studies, in a recent review, Piani et al. (2022a) collected 11 fMRI "Go/No-Go" studies involving the MDD population. They showed that the correlation between behavioral data and diagnosis is controversial and that MDD presented higher activations in the central prefrontal cortex and right superior temporal gyrus (STG), lower activations in the left STG and thalamus, and mixed results in the IPG and ACC, compared to HC. The study showed changes in regions involved in sustained attention, typically impaired in MDD subjects. Inconsistency reported in the findings could be related to age- (Zhang et al., 2016; Katz et al., 2010; Vallesi, 2011) and sex-related (Piani et al., 2022b) effects or severity of depression (Quinn et al., 2012). Similar results were shown for late-life MDD, with a lower activation of N2 components in ACC during the task compared to healthy subjects (Katz et al., 2010).

Most studies investigating inhibitory control processes in HC and MDD were unimodal. However, using a single modality to investigate this process could represent a limit, concealing specific areas or networks of interest. Thus, there is a need to combine different techniques for exploiting the strengths of each modality. Specifically, the combination of the high temporal resolution of the EEG and the high spatial resolution of the fMRI could lead to unveiling the neural underpinning of processes of interest (Mulert et al., 2008; Huster et al., 2010; Jorge et al., 2014; Karch et al., 2014; Maggioni et al., 2016; McMillan et al., 2020). When EEG and fMRI are recorded simultaneously, the same physiological conditions are guaranteed, and the real-time associations between EEG events of interest and hemodynamic fluctuations can be explored; however, the concurrent recording of EEG inside the MR machine provides technological issues that need to be addressed carefully (Maggioni et al., 2014; Bullock et al., 2021). A few studies investigated the inhibitory control in healthy subjects using the ERP peaks to drive the fMRI analysis (Huster et al., 2010; Baumeister et al., 2014; Iannaccone et al., 2015), whereas none has combined EEG and fMRI to explore this process in MDD.

For the first time, this study investigates the neurovascular bases of inhibitory control in older adults with late-onset MDD, compared to healthy controls, through simultaneous EEG-fMRI during a visuomotor Go/No-Go task. By leveraging EEG high temporal resolution and fMRI high spatial resolution, using an EEG-driven fMRI approach, we aim to investigate distinct cognitive stages of inhibitory control, represented by N2 and P3 ERP peaks. We hypothesize that MDD will exhibit altered hemodynamic responses compared to HC in brain regions associated with conflict monitoring (N2) and response inhibition (P3). These changes are expected to highlight both commonalities and distinctions in the neural mechanisms underlying inhibitory control between MDD and HC, thereby advancing our understanding of depression-related cognitive dysfunctions.

2. Materials and methods

We used the STROBE cross sectional checklist when writing our report (Elm et al., 2014).

2.1. Dataset

The dataset was collected from forty-four subjects, nineteen affected by MDD and twenty-five HC, all right-handed. The sample included 6 pairs of twins; the sibling who showed worse task performances was excluded in each pair. Patients were diagnosed with MDD using the Italian version of the Structured Clinical Interview for DSM-5 (SCID), and only subjects with late-onset MDD ($\geq$ 45 years) were included. Exclusion criteria for all participants comprised lifetime alcohol or substance abuse, whereas additional exclusion criteria for patients were current DSM-5 comorbid psychiatric disorders and lifetime psychotic

symptoms. The dataset included demographic, clinical, cognitive, and multimodal brain data. The clinical assessment included the Hamilton Depression Rating Scale (HDRS) (Hamilton, 1960), the treatment, the repeatable battery for assessment of neuropsychological status (RBANS) (Randolph et al., 1998), and the Frailty Index (Bersani et al., 2020). The research protocol was approved on the 13th of April 2018 by the Ethical Committee of the Fondazione IRCCS Ca' Granda Ospedale Maggiore Policlinico, Milan, Italy (238_2018bis). All participants signed an informed consent to the study protocol.

2.2. Experimental design

The EEG-fMRI protocol consisted in a visuomotor Go/No-Go task, already presented in Piani et al., (2022b), that was implemented using Presentation® software (Neurobehavioral Systems, Inc., Berkeley, CA, USA). The protocol comprised four excitatory blocks ("Go" blocks) containing only target stimuli and four inhibitory blocks ("Go/No-Go" blocks) containing both target and non-target stimuli. In "Go" blocks, subjects were required to push a button with their right thumb when red or green squares appeared on the screen, instead in "Go/No-Go" blocks, they were asked to press the button only in front of green squares and suppress their response in front of red squares. Following an initial rest interval of 16 s, each block lasted 32 s and was followed by a rest interval (with a fixation cross at the center of the screen) of 16 s. The total task duration was 400 s. The condition configuration was the same for all subjects. The stimulation blocks were synchronized to the fMRI volumes using the NordicNeuroLab SyncBox (NNL, Bergen, Norway) and delivered through the MR-compatible NNL VisualSystem HD. The MR-compatible NNL ResponseGrip device, composed of thumb and index finger buttons, was used to collect participants' responses. The participants with a percentage of incorrect task responses (response for non-target stimuli and lack of it for target ones) greater than 35 % were excluded.

2.3. Data acquisition

EEG data were recorded simultaneously with fMRI using an MR-compatible EEG system (Geodesic EEG system 400, Electrical Geodesic Inc., USA) equipped with a cap including 64 EEG channels and 1 electrocardiographic (ECG) channel (Hydrocel Geodesic Sensor Net HCGSN v.1.0, Electrical Geodesic Inc., USA). The EEG sampling frequency (fs) was 1000 Hz, and the reference electrode was placed at the intersection between the nasion-inion distance and the preauricular distance. The impedance at each electrode was kept lower than 50 kΩ.

MRI acquisitions were performed using a 3T Philips Achieva DStream scanner (Philips, Best, The Netherlands) with a 32-channel head coil. Two hundred (plus two dummy) fMRI volumes were collected during the task using a multi-transmit T2*-weighted echo planar imaging sequence (field of view (FOV) = 120 mm (FH) × 256 mm (AP) × 256 mm (RL), voxel size = 2 × 2 × 2 mmˆ3, echo time (TE) = 30 ms, repetition time (TR) = 2000 ms, flip angle = 90°). Five additional (plus two dummy) fMRI scans were acquired with the same parameters but opposite phase encoding direction and used to estimate and correct for susceptibility-induced distortions in the fMRI volumes. To provide a morphological reference for fMRI data, structural T1-weighted images were collected using a 3D turbo field echo SENSE sequence (FOV = 250 mm (FH) × 240 mm (AP) × 180 mm (RL), voxel size = 1 mmˆ3, TE = 4 ms, TR = 8 ms, flip angle = 8°).

2.4. EEG pre-processing

EEG data were first processed using EEGLAB, an open-source toolbox running in MATLAB® 2022a (The Mathworks, Inc., Natick, Massachusetts, USA) (Delorme and Makeig, 2004). The gradient artifact was firstly removed by subtracting a template, generated from a sliding average of 21 blocks of the artifact, from each channel (Allen et al., 1998). Subsequently, all channel time series were downsampled to 250 Hz (anti-aliasing filtering at a cutoff frequency of 90 % of the Nyquist frequency), and filtering of EEG (0.1–70 Hz and notch at 50 Hz) and ECG (0.1–30 Hz) channels was performed. Pulse artifacts (PAs) were removed with BrainVision Analyzer 2.0 (BrainProducts, Gilching, Germany), identifying semiautomatically the R peaks and using them as markers for PA occurrence (Allen et al., 2000). Bad intervals were marked based on visual inspection, whereas eye movements, muscular artifacts, and remaining PAs were removed by applying an extended Infomax ICA (Mayeli et al., 2016; Maggioni et al., 2014). Lastly, the EEG signal was re-referenced to the average of all channels, low-pass filtered at 30 Hz, and visually inspected for residual bad intervals, which were marked (see Fig. S1 for preprocessing results). Data were segmented into stimulus epochs according to the stimulus type (target "Go" blocks, target "Go/No-Go" blocks, and non-target "Go/No-Go" blocks) from −200 ms before to 600 ms after the stimulus. Epochs previously marked as bad intervals, target stimulus epochs without any response or response after more than 600 ms, and non-target stimulus epochs with a response were removed (Jia et al., 2017; Reed et al., 2013). The artifact-free epochs were averaged per stimulus condition (target "Go" blocks, target "Go/No-Go" blocks, and non-target "Go/No-Go" blocks) for each participant, obtaining the ERP waves. N2 and P3 were searched in the frontal region ERP waves as the greatest negative and positive peaks in the time windows [150–250 ms] and [200–500 ms], respectively (Falkenstein et al., 1999; Polich, 2007). Considering the entire population, the electrodes of interest (EOI) were selected searching for the "Go/No-Go" N2 and "Go/No-Go" P3 effects (Falkenstein et al., 1999; Pfefferbaum et al., 1985), comparing target and non-target ERPs of "Go/No-Go" blocks using a Wilcoxon signed rank test ($p < 0.05$). For each subject and stimulus condition, the ERP and single-trial amplitudes and latencies of N2 and P3 peaks at EOI were extracted as features.

2.5. fMRI pre-processing

fMRI data were pre-processed using MATLAB® 2022a, the Statistical Parametric Mapping (SPM) software (version 12) (Penny et al., 2007) and the FMRIB Software Library (FSL) software (version 6) (Jenkinson et al., 2012). The pre-processing steps were: (1) realignment to the first image, (2) susceptibility-induced distortions' artifact correction using the topup tool of FSL, (3) co-registration with the T1-weighted image, (4) normalization according to Montreal Neurological Institute (MNI) standard space, and (5) spatial smoothing using a 4 mm size full width half maximum 3D Gaussian kernel.

2.6. Behavioral and ERP analysis

The response time (RT) and the percentage of correct responses were extracted as the task performance indicators. A GLM analysis ($p < 0.05$) was used to assess the effect of the diagnosis on those variables, considering age and sex as covariates (variable ~ 1 + diagnosis + age + sex). The ERP features extracted in the "Go/No-Go" blocks (N2 and P3 latencies and amplitudes) were tested for diagnosis-by-inhibition effects (target vs. non-target) using a GLM analysis ($p < 0.05$), adding age, sex, and subject factor as covariates (variable ~ 1 + diagnosis*task + age + sex + subject).

2.7. EEG-driven fMRI analysis

This integrated analysis (Fig. 1) aimed at extracting the fMRI responses to N2 and P3 ERP components separately. The first-level analyses were conducted using two GLM design matrices to extract N2 and P3 activation maps, separately. For each GLM, the voxel-based fMRI time series (dependent variables) were modeled in terms of task-related ERP responses and confounding factors (independent variables). Specifically, each design matrix included three ERP regressors (one for each stimulus type, i.e., target "Go" blocks, target "Go/No-Go" blocks, and

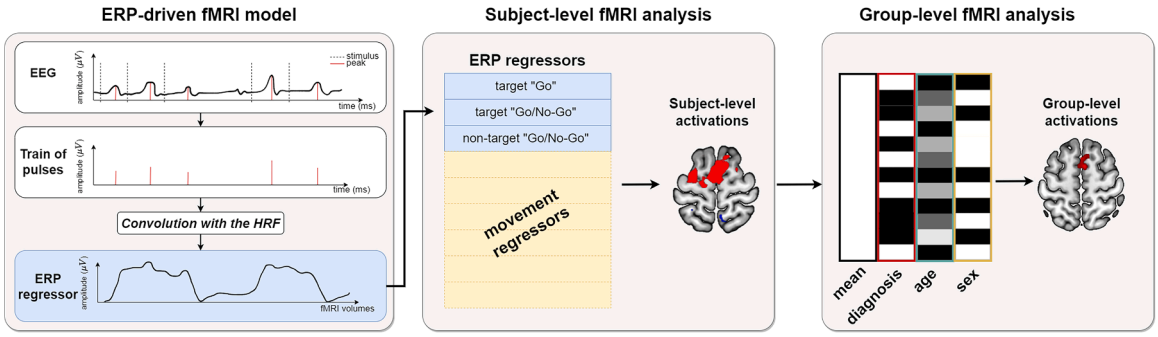

Fig. 1. EEG-driven fMRI analysis pipeline. After EEG pre-processing and channel selection, an ERP regressor is built for each peak and stimuli condition. The ERP regressor is built by convolving the HRF with a train of pulses modulated with amplitude and latency of single-trial peaks. Subsequently, the ERP regressor is downsampled (fs=0.5 Hz) and entered in the GLM design matrix, along with the movement regressors. The GLM design matrix is fitted to the subject's voxel-based fMRI data obtaining subject-level activation maps. Maps are used for the second-level analysis using a GLM model with diagnosis, sex, and age as covariates. *ERP: event-related potentials; HRF: Hemodynamic Response Function; fs: sampling frequency; GLM: general linear model.*

non-target "Go/No-Go" blocks) and six movement regressors (three for head translation and three for head rotation) extracted from the fMRI pre-processing pipeline. Each ERP regressor (N2 or P3) was constructed as follows (Fig. 1): (1) single-trial amplitudes and latencies of the relative peak of interest were extracted from their respective time window and EOI, (2) delta functions were set at the single-trial peak latencies and modulated for the relative single-trial amplitudes, (3) the amplitudes with values beyond ± 3 SD (standard deviation) were substituted with the mean of the amplitudes within 3 SD, (4) the absolute values were taken to build the regressor, and lastly (5) convolved with the canonical hemodynamic response function (HRF) and downsampled to match the fMRI sampling frequency (fs = 0.5 Hz). Each GLM matrix, one for N2 and one for P3, was fitted to the subject's voxel-based pre-processed fMRI data, obtaining first-level fMRI contrast maps for the following t-contrasts: (1) target "Go" vs. rest, (2) target "Go/No-Go" vs. rest, (3) non-target "Go/No-Go" vs. rest, (4) target vs. non-target "Go/No-Go", and (5) target "Go" vs. target "Go/No-Go". To examine brain activations associated with each stimulus type relative to baseline, the "stimulus type vs. rest" contrast (e.g., target "Go" vs. rest, target "Go/No-Go" vs. rest, non-target "Go/No-Go" vs. rest) was used, allowing to identify brain regions responding to different stimulus conditions. Moreover, to isolate neural mechanisms related to inhibitory processing, the contrast between target and non-target stimuli within "Go/No-Go" blocks were examined, to reveal differences in brain activation when subjects must execute a response (target) versus when they must inhibit a response (non-target) in the same inhibitory context (i.e., inhibitory blocks). Finally, following Criaud et al. (2013), we investigated the contrast between target stimuli in excitatory versus inhibitory blocks (target "Go" vs. target "Go/No-Go"). This comparison highlights differences in target processing between contexts where responses are always executed (excitatory blocks) and contexts where response inhibition might be required (inhibitory blocks), thereby revealing attentional and preparatory processes unique to the inhibitory context. The first-level fMRI contrast maps were then inserted in a second-level random--effects GLM analysis. For each contrast, a GLM design using the contrast maps as dependent variables, and diagnosis, age, and sex as independent variables was employed. Other potential confounders, including medication, were not considered for the limited size of the sample. However, a supplementary analysis has been performed on the MDD group investigating the effect of depressive symptoms, measured using HDRS, on brain activation at net of age and sex. Results are reported in Supplementary Tables S1 and S2. After GLM estimation, t-contrasts were employed to assess group-level positive and negative responses and diagnosis effects, at net of age and sex. The significant clusters were localized based on the AAL atlas (Rolls et al., 2020).

3. Results

Among the forty-four participants with EEG-fMRI data, two were excluded for bad performances (percentage of correct answers below 65 %) and one sibling for each pair of the six twins was discarded. Therefore, the final dataset was formed by 18 subjects affected by MDD (9F, 9 M, 70 ± 11 years old) and 18 healthy volunteers (10F, 8 M, 69 ± 24 years old), whose demographic, clinical, and behavioural characteristics are reported in Table 1. Sex ($p = 1$), age ($p = 0.87$, $Z = -0.16$), RBANS ($p = 0.93$, $Z = 0.08$), and Frailty Index ($p = 0.24$, $Z = 1.18$) distributions were comparable between the two groups, when using respectively

Table 1
Demographical and behavioural variables.

	MDD (N = 18)	HC (N = 18)	Stats (MDD vs. HC)
Demographic			
Sex [N]	9F, 9M	10F, 8M	pval=1
Age [years]	70 (11)	69 (24)	pval=0.87, Z-value = −0.16
HDRS score	9 (8)	1 (6)	**pval=0.0015, Z-value = 3.18**
Antidepressant [N]	11	0	–
SSRI [N]	9	–	
SNRI [N]	1	–	
Vortioxetina [N]	1	–	
Antidepressant and other drugs [N]	9	2	–
Other drugs [N]	3	3	–
No drugs [N]	4	13	–
RBANS *	98.0 (21.5)	97.5 (17.0)	pval=0.93, Z-value=0.08
Frailty Index ^	0.18 (0.17)	0.08 (0.23)	pval=0.24, Z-value=1.18
Behavioural			
target "Go" resp time [ms]	281.97 (62.60)	287.63 (75.69)	pval=0.25, T = 1.17
target "Go" correct resp [%]	92.58 (19.51)	95.31 (5.52)	**pval=0.02, T=−2.55**
target "Go/No-Go" resp time [ms]	337.77 (71.63)	303.97 (50.56)	**pval=0.02, T = 2.48**
target "Go/No-Go" correct resp [%]	88.94 (22.33)	94.68 (6.82)	**pval=0.02, T=−2.29**
non-target "Go/No-Go" no resp [%]	79.17 (12.50)	79.17 (25.00)	pval=0.87, T=−0.17

Median (interquartile ranges) are reported for age, HDRS, RBANS, Frailty Index, and behavioural variables. For the statistical comparison between the two groups, Fisher's test was used for sex, Mann–Whitney test was used for age and HDRS, RBANS, and Frailty Index scores, whereas general linear models were used to assess the effect of diagnosis on the behavioural variables, correcting for age and sex. * available for 16/18 MDD and 14/18 HC; ^ available for all MDD and 14/18 HC.

Fisher's test for sex and Mann-Whitney test for the other variables. In contrast, using the Mann-Whitney test, the HDRS scores resulted statistically different between the two groups ($p = 0.0015$, $Z = 3.18$). The GLM analysis on the behavioural variables showed differences between the two groups in (i) RT of target stimuli in "Go/No-Go" blocks ($p = 0.02$, $T = 2.48$) and (ii) the percentage of correct responses to target stimuli in both "Go" ($p = 0.02$, $T=-2.55$) and "Go/No-Go" blocks ($p = 0.02$, $T=-2.29$).

3.1. ERP

The pool of E6 (Fz), E9 (F1), and E3 (F2) were selected as electrodes of interest according to the "Go/No-Go" N2 and "Go/No-Go" P3 effects. One exemplar ERP per group is shown in Fig. 2. The ERPs and single-trial N2 and P3 were consequently searched at the pool of Fz-F1-F2 in the previously defined time windows. The peak amplitudes and latencies, and the relative GLM results, are reported in Table 2 and Table 3, respectively. Specifically, the inhibitory effect (|non-target| > |target| in "Go/No-Go" blocks) was found for N2 amplitude ($p = 0.002$, $T=-3.38$) and for P3 amplitude ($p = 0.003$, $T = 3.18$) and latency ($p = 0.023$, $T = 2.39$); N2 ($p = 0.001$, $T = 3.56$) and P3 ($p = 0.002$, $T = 3.35$) latencies showed a diagnosis effect. No variables showed a significant diagnosis*inhibitory interaction effect.

3.2. EEG-driven fMRI

The significant results ($p < 0.001$, cluster-based thresholding using $k = 15$, corrected for non-isotropic smoothness) of the EEG-driven fMRI maps are reported below separately for N2 (Table 2) and P3 (Table 3). The positive and negative group-level activation on task (vs. rest) contrasts for N2 and P3 are reported in Tables S3 and S4, respectively.

3.2.1. N2 regressors

Target stimuli in "Go/No-Go" blocks (vs. non-target in "Go/No-Go" blocks) showed higher activation of the bilateral paracentral lobule and right SMA. Whereas the target "Go/No-Go" stimuli (vs. target in "Go" blocks) showed a higher activation of portions of the vermis, left cerebellum, left STG and middle temporal gyrus (MTG), and right IPG, and a lower deactivation of the left precuneus (Fig. 3).

Significant effects of the diagnosis were observed in the target "Go/No-Go" stimuli (vs. rest), showing a higher activation in the MDD group of the left IPG and left precentral and postcentral gyri (positive BOLD response for MDD and negative BOLD response for HC), whereas a higher activation in the HC group of the left thalamus (positive BOLD response for HC and negative BOLD response for MDD) was found. In non-target "Go/No-Go" stimuli (vs. rest), MDD showed higher activation of the left STG (positive BOLD response for MDD and negative BOLD response for HC).

The left STG was also more activated in HC (vs. MDD) in the target "Go/No-Go" stimuli (vs. non-target in "Go/No-Go" blocks); specifically, the left STG in HC was more active in the target stimuli with respect to non-target stimuli (inhibitory blocks), whereas in MDD it showed an

Table 2
ERPs amplitudes.

	target "Go" block		target "Go/No-Go" block		non-target "Go/No-Go" block	
	N2 (μV)	P3 (μV)	N2 (μV)	P3 (μV)	N2 (μV)	P3 (μV)
HC	−0.02 (3.16)	6.34 (5.03)	−1.17 (4.70)	4.07 (6.47)	−4.10 (10.68)	7.66 (7.38)
MDD	−0.92 (4.67)	4.24 (3.60)	−0.76 (3.42)	4.67 (4.27)	−3.86 (3.83)	8.10 (9.92)
GLM	–	–	Inhibitory effect (pval=0.002, $T=-3.38$)	Inhibitory effect (pval=0.003, $T = 3.18$)	–	–

ERP N2 and P3 amplitude for stimulus types and groups [median (interquartile range)]. The inhibitory effect is reported (GLM, $p < 0.05$) when target and non-target stimuli in the inhibitory block are compared considering age, sex, and subject factor as covariates.

Table 3
ERPs latencies.

	target "Go" block		target "Go/No-Go" block		non-target "Go/No-Go" block	
	N2 (ms)	P3 (ms)	N2 (ms)	P3 (ms)	N2 (ms)	P3 (ms)
HC	190 (36)	328 (164)	198 (56)	330 (172)	206 (60)	426 (116)
MDD	210 (72)	388 (204)	196 (36)	322 (108)	184 (32)	390 (188)
GLM	–	–	Diagnosis (pval=0.001, $T = 3.56$)	Diagnosis (pval=0.002, $T = 3.35$), Inhibitory effect ($p = 0.023$, $T = 2.39$)	198 (56)	198 (56)

ERP N2 and P3 latency for stimulus types and groups [median (interquartile range)]. The inhibitory and diagnosis effects are reported (GLM, $p < 0.05$) when target and non-target stimuli in the inhibitory block are compared considering age, sex, and subject factor as covariates.

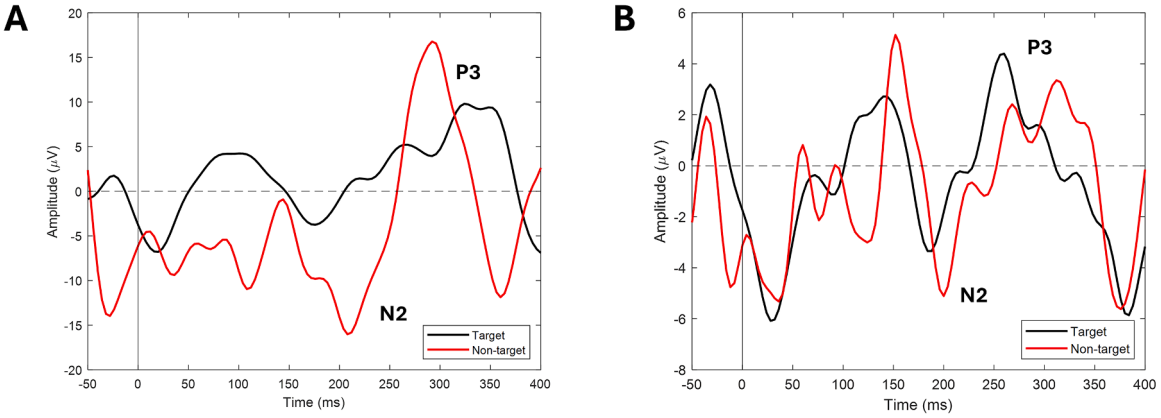

Fig. 2. ERP waveforms. ERP waveforms in response to target (black) and non-target (red) stimuli in "Go/No-Go" blocks for an exemplary HC (A) and MDD (B) showing N2 and P3 components. *ERP: Event-related Potentials; HC: healthy controls; MDD: major depressive disorder.*

Table 4
N2-driven fMRI activation maps.

Effect	Contrast	T-stat	# voxels	x, y, z	Overlap	AAL regions	p
Negative BOLD response	target "Go/No-Go" > non-target "Go/No-Go"	4.42	21	34 −22 32	100 %	Unknown	$p < 0.001$, $k = 15$
		4.32	15	4 −38 66	80 %	Paracentral Lobule R	
					13 %	Unknown	
					7 %	Precuneus L	
		3.97	12	4 −22 60	92 %	Supp Motor Area R	
					8 %	Paracentral Lobule L	
Negative BOLD response	target "Go" > target "Go/No-Go"	5.06	34	−12 −48 54	85 %	Precuneus L	$p < 0.001$, $k = 15$
					12 %	Unknown	
					3 %	Cingulum Mid L	
		5.04	7	−50 −46 18	71 %	Temporal Sup L	
					29 %	Temporal Mid L	
		4.80	29	−2 −52 −20	72 %	Vermis 4 5	
					17 %	Cerebelum 4 5 L	
					10 %	Vermis 3	
		4.45	17	42 −46 50	100 %	Parietal Inf R	
MDD > HC	target "Go/No-Go"	4.87	22	−38 −52 36	73 %	Parietal Inf L	$p < 0.001$, $k = 15$
					27 %	Angular L	
		4.54	16	−28 −26 50	56 %	Unknown	
					31 %	Precentral L	
					12 %	Postcentral L	
MDD > HC	non-target "Go/No-Go"	4.51	18	−58 −38 18	100 %	Temporal Sup L	$p < 0.001$, $k = 15$
MDD > HC	target "Go" > target "Go/No-Go"	4.30	18	48 −26 4	100 %	Temporal Sup R	$p < 0.001$, $k = 15$
HC > MDD	target "Go/No-Go"	5.74	7	−16 −12 2	100 %	Thalamus L	$p < 0.001$, $k = 15$
HC > MDD	target "Go" > target "Go/No-Go"	4.49	28	20 −66 −16	96 %	Cerebelum 6 R	$p < 0.001$, $k = 15$
					4 %	Lingual R	
HC > MDD	target "Go/No-Go" > non-target "Go/No-Go"	4.25	14	−58 −38 18	100 %	Temporal Sup L	

EEG-driven fMRI significant results ($p < 0.001$, cluster corrected for non-isotropic smoothness, $k = 15$), for N2 regressor are reported in this table. The table reports the effect, contrast, T-stat relative to each cluster, number of voxels within each cluster, the MNI coordinates of the cluster peak, percentage of overlap and relative AAL region.

Table 5
P3-driven fMRI activation maps.

Effect	Contrast	T-stat	# voxels	x, y, z	Overlap	AAL regions	p
Negative BOLD response	target "Go" > target "Go/No-Go"	5.04	33	−2 −54 −22	88 %	Vermis 4 5	$p < 0.001$, $k = 15$
					9 %	Cerebelum 4 5 L	
					3 %	Vermis 3	
		4.65	23	2 −48 54	83 %	Precuneus R	
					17 %	Precuneus L	
		4.61	46	34 6 48	74 %	Frontal Mid R	
					26 %	Precentral R	
		4.60	44	−6 16 50	100 %	Supp Motor Area L	
		4.56	20	−16 −8 18	75 %	Unknown	
					20 %	Thalamus L	
					5 %	Caudate L	
		4.50	17	10 −50 −20	94 %	Cerebelum 4 5 R	
					6 %	Vermis 4 5	
MDD > HC	target "Go/No-Go"	4.56	31	−42 −50 36	77 %	Parietal Inf L	$p < 0.001$, $k = 15$
					13 %	Angular L	
					10 %	SupraMarginal L	
		4.49	26	−46 −6 8	92 %	Rolandic Oper L	
					8 %	Heschl L	
MDD > HC	target "Go" > target "Go/No-Go"	4.42	16	32 −8 −10	75 %	Unknown	$p < 0.001$, $k = 15$
					25 %	Putamen R	

EEG-driven fMRI significant results ($p < 0.001$, cluster corrected for non-isotropic smoothness, $k = 15$), for P3 regressor are reported in this table. The table reports the effect, contrast, T-stat relative to each cluster, number of voxels within each cluster, the MNI coordinates of the cluster peak, percentage of overlap and relative AAL region.

opposite behavior. Lastly, the target "Go" stimuli (vs. target in "Go/No-Go" blocks) showed a higher activation in MDD (vs. HC) of the right STG and a higher activation in HC (vs. MDD) of the right cerebellum.

3.2.2. P3 regressors

Target stimuli in "Go/No-Go" blocks (vs. target in "Go" blocks) showed a more positive BOLD response of the vermis, bilateral cerebellum, right middle frontal and precentral areas, left SMA and thalamus, and a less negative BOLD response of the bilateral precuneus.

Significant diagnosis effects were observed in target "Go/No-Go" stimuli (vs. rest) in the left rolandic operculum, Heschl's, IPG, angular, and supramarginal areas, which showed a positive BOLD response in MDD, and a negative BOLD response in HC (Fig. 4). The same trend was observed for the right putamen when target "Go" stimuli were compared to target "Go/No-Go" stimuli.

4. Discussion

The present study proposed and applied a multimodal analysis framework for exploring the neurovascular brain correlates of different stages of inhibitory control in older adults with late-onset MDD and controls. Despite being preliminary, our findings suggest an altered

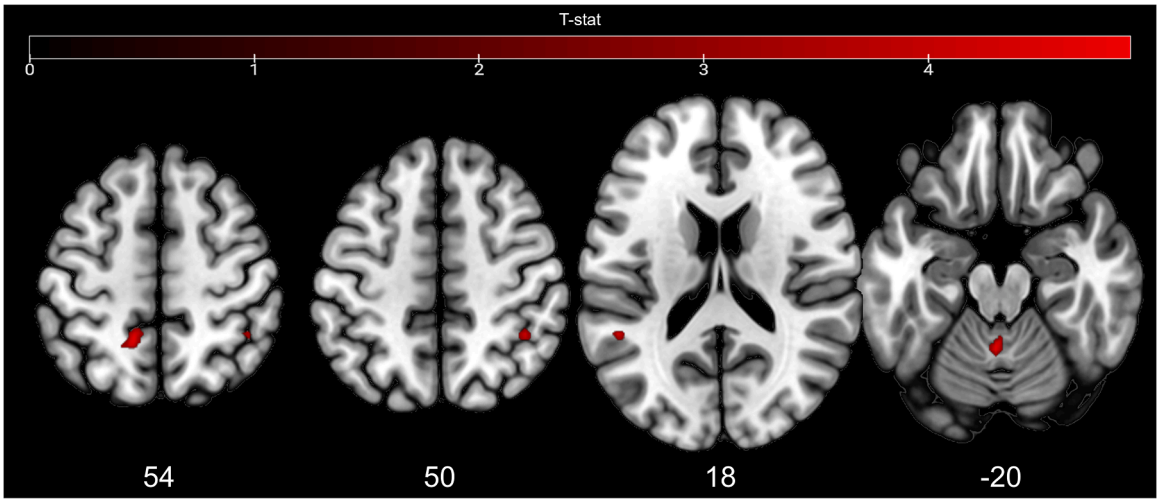

Fig. 3. EEG-driven fMRI results using N2 as regressor for target "Go/No-Go" > target "Go". Results of negative BOLD activation of contrast target "Go" > target "Go/No-Go" ($p < 0.001$, cluster-based thresholding using $k = 15$, corrected for non-isotropic smoothness). Significant clusters include left precuneus (slice $z = 54$, peak: −12, −48, 54), right inferior parietal (slice $z = 50$, peak: 42, −46, 50), left middle and superior temporal gyrus (slice $z = 18$, peak: −50, −46, 18), and vermis and left cerebellum (slice z=−20, peak: −2, −52, −20). All coordinates are in MNI space. Complete cluster statistics are provided in Table 4. The significant BOLD responses are overlaid over a canonical image (mni152) template using MRIcroGL software (https://www.nitrc.org/projects/mricrogl). *BOLD: blood oxygen level dependent.*

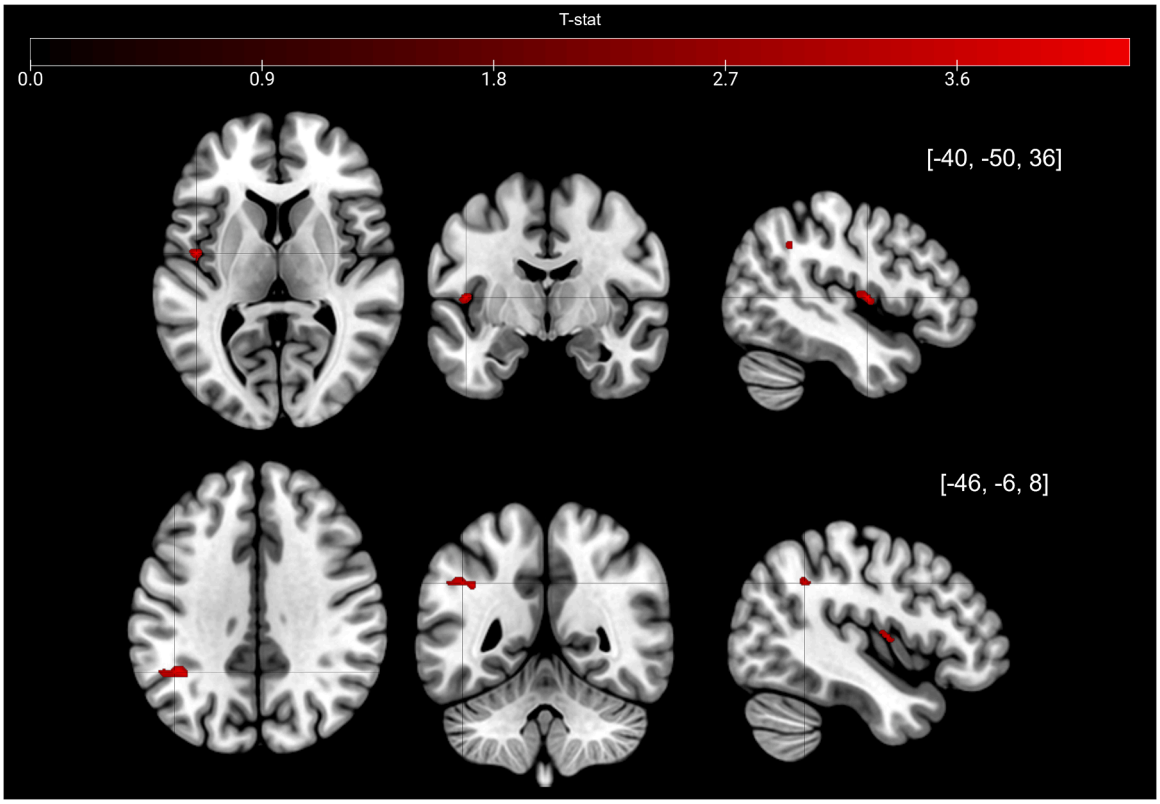

Fig. 4. EEG-driven fMRI results using P3 as regressor for target "Go/No-Go" > rest for diagnosis effect. Results of diagnosis effect (MDD > HC) of contrast target "Go/No-Go" (vs. rest) ($p < 0.001$, cluster-based thresholding using $k = 15$, corrected for non-isotropic smoothness). The statistical analysis showed the activation of left inferior parietal, supramarginal, and angular region (upper row, peak: −42, −50, 36), and left rolandic and heschl (lower row, peak: −46, −6, 8). All coordinates are in MNI space. Complete cluster statistics are provided in Table 5. The significant BOLD responses are overlaid over a canonical image (mni152) template using MRIcroGL software (https://www.nitrc.org/projects/mricrogl). *MDD: major depressive disorder; HC: healthy controls; BOLD: blood oxygen level dependent.*

involvement of cortical and subcortical brain regions in multiple stages of cognitive control in affected individuals. Studies in MDD reported mixed findings regarding inhibitory control, with some (Dai and Feng, 2011; Joormann et al., 2007) suggesting that MDD patients have insufficient inhibition of irrelevant negative information into the working memory, resulting in the interference with relevant positive or neutral information. In general, working memory and sustained attention are compromised in MDD patients, and a recent study (Piani et al.,

2022a) suggested altered functional changes in those regions involved in cognitive activities responsible for response inhibition. However, the major limitation of previous studies is the application of a single modality to investigate this process. The possibility of simultaneously combining different modalities and exploiting the advantages of the different techniques in the same experimental conditions might help greatly unveil the brain mechanisms underlying response inhibition and its role in MDD. Here, for the first time, we coupled EEG and fMRI in a Go/No-Go task to explore multiple stages of the response inhibition process in older people with late-onset MDD compared to healthy older adults. We deliberately focused on the late stage of the lifespan, which is known to be characterized by emphasized depression-related cognitive decline (Dotson et al., 2020).

Given the strengths and weaknesses of the two methods, combining them has the potential to disentangle the different neurovascular processes involved in the inhibition process during a Go/No-Go task, providing insights into brain function that cannot be measured by a single modality. Obtaining simultaneous EEG-fMRI has several advantages (Warbrick, 2022) as the need of a single recording session, which is particularly valuable in scenarios where separate sessions would not be able to capture the same activity, such as in cognitive tasks; moreover, it allows having the same sensory environment for all measures (sitting in a lab versus lying in a noisy scanner), therefore reducing the confounding variables of the experiment, and also reduces habituation effects. This multimodal approach has already given interesting results in the general population (Debener et al., 2005, 2006; Mayhew et al., 2013; Maggioni et al., 2016). For the first time, we applied combined EEG-fMRI to a Go/No-Go task in patients affected by late-onset MDD, a population underrepresented in prior research, proving that this approach is also feasible in a clinical sample. Moreover, the multimodal approach allowed us to capture both temporal and spatial dynamics of neural activity, providing a comprehensive view of cognitive sub-processes that is not achievable with unimodal methods. Our findings demonstrate the ability to disengage distinct stages of inhibitory control and identify diagnostic-specific neural signatures, advancing the field's understanding of cognitive dysfunctions in MDD.

Previous studies investigating Go/No-Go tasks, found fMRI inhibitory control correlates in the frontal cortex, IPG, precuneus, SMA, pre-SMA, and insula (Swick et al., 2011; Simmonds et al., 2008; Criaud and Boulinguez, 2013). However, these unimodal studies did not differentiate between different cognitive sub-processes. We aim to differentiate between different sub-processes of inhibitory control in a visuomotor Go/No-Go task, further investigating the differences related to depression disorder. In our study, common activations between N2 and P3 regressors, when comparing target "Go/No-Go" stimuli with target "Go" stimuli in the entire population, were found in areas previously reported as involved in the inhibitory control, such as the SMA, precuneus, cerebellum (Swick et al., 2011; Simmonds et al., 2008; Criaud and Boulinguez, 2013; Mannarelli et al., 2020), and also in the vermis. Moreover, the EEG-driven fMRI approach was able to differentiate between separate inhibitory control stages investigating N2 and P3 hemodynamic correlates and delving into differences between HC and MDD. The N2 component, occurring approximately 200–300 ms post-stimulus, is primarily associated with conflict monitoring and the initial detection of response conflict when competing responses are activated simultaneously, representing the first stage of inhibitory control (Falkenstein et al., 1999; Bokura et al., 2001; Enriquez-Geppert et al., 2010). In contrast, the P3 component, appearing around 300–500 ms post-stimulus, reflects the implementation of inhibitory control and response evaluation processes, reflecting the second stage of inhibition, more closely aligned with the actual suppression of motor responses (Polich, 2007; Garavan et al., 1999). In the next paragraphs, we will focus on the regions that were found uniquely for N2 and P3 regressors and on the differences showed in the different inhibition stages between the two groups.

4.1. N2 results

In classic EEG studies, N2 responses have traditionally been associated with the inhibition of motor responses during Go/No-Go tasks, reflecting the final stages of automatic processes and being associated with cognitive control and response inhibition (Zhang et al., 2023). Specifically, N2 is related to attention allocation during conflict monitoring when two or more incompatible responses are simultaneously activated (Wauthia and Rossignol, 2016).

In our study, N2 was associated with several fMRI activations in the entire population. The comparison between target "Go/No-Go" stimuli (vs. target "Go" stimuli) showed a greater BOLD response, uniquely associated with N2, of left STG and MTG, and right IPG area. Moreover, the comparison between target and non-target stimuli in "Go/No-Go" blocks showed higher activation of the bilateral paracentral lobule and right SMA in non-target stimuli. These results were in line with previous studies (Swick et al., 2011; Simmonds et al., 2008; Criaud and Boulinguez, 2013), specifically the temporal activation related to N2 regressor in inhibitory control, which was also found by Iannaccone et al. (2015) and Baumeister et al. (2014). However, unlike previous studies, we did not find significant activation related to the N2 peak in the frontal, insula, thalamic, and cingulate regions.

Besides commonalities between the two groups, alterations in the MDD were found in the right STG and right cerebellum when target "Go" stimuli were compared to target "Go/No-Go" stimuli. A recent study in HC showed that cerebellar areas are important to allocating attentional resources to stimuli containing conflict information and to inhibitory control (Mannarelli et al. 2020). Mannarelli and colleagues inhibited cerebellum by means of tDCS and showed a reduction in N2-No-Go amplitude and a prolongation in N2-No-Go latency, indicating that the orienting and initial discrimination of the incongruous stimulus are delayed. The No-Go stimulus, which informs the subject to withhold the motor response, is by definition, an incongruent stimulus and is thus able to activate an orienting response. The orienting response toward an incongruent stimulus usually involves frontal-parietal brain areas in the ventral attention network, which identifies salient changes in the environment and acts as an alert system or circuit-breaker for the dorsal attention system (Mannarelli et al., 2020). The aforementioned areas present connections, through the thalamus, with the basal ganglia and the cerebellum (Bostan et al., 2013), which is believed to regulate the level of activation or inhibition and manage the timing, speed, and appropriateness of cognitive processes, especially through an inhibitory pathway (Bostan et al., 2013). Regarding mood disorders, cerebellum seems also to play a role in suicidal behaviors. Functionally, recent studies suggested involvement of the cerebellum in the recollection of memories related to suicide attempts. In a recent publication (Shaffer et al., 2022), participants who had attempted suicide had greater fMRI task-related activation in visual areas and the cerebellum, with the number of suicide attempts associated with the difference in BOLD response. This involvement in suicide might be related to the circuit of emotional pain (Pigoni et al., 2025). Recent studies (Tymofiyeva et al., 2023) proposed a two-circuit model in shaping suicide risk: the emotional pain circuit, including the cerebellum, hippocampus, and amygdala, and the social disconnect circuit, which comprises the lateral OFC and temporal gyri, as well as the connections between them (the frontotemporal system). Given this hypothesis, the role of cerebellum in conflict monitoring and response inhibition might also have practical implications in the management of at-risk patients. Moreover, the STG has been implicated in the pathogenesis of MDD, showing reduction in GM (Kandilarova et al., 2019) and alterations in functional activity (Li et al., 2022), in both current and remitted MDD patients (Takahashi et al., 2010; Zhao et al., 2023). From a functional point of view, the STG is part of the DMN, which has been reported altered in MDD patients that have the tendency to indulge more in psychological activity of self-reference (Kaiser et al., 2003). Moreover, it participates in emotional and high-level cognitive functions such as emotional

attention and social cognition (Narumoto et al., 2001). In a recent fMRI study, during response inhibition task the attenuation of connectivity in the precentral and bilateral STG correlated with post treatment symptom improvement after sertraline treatment (Tozzi et al., 2020), suggest a possible role as a marker of response. Finally, regarding depression, studies showed that alterations in activation in parietal (Richard-Devantoy et al., 2016) and cingulate areas (Richard-Devantoy et al., 2016; Malejko et al., 2021) during a Go/No-Go task correlate with psychological pain, suicidal and self-harm ideation, and global functioning as well. Our results showed alterations in MDD in target "Go/No-Go" stimuli (vs. rest) in the left parietal, sensorimotor cortex, and thalamus regions. These results are in line with the aforementioned studies and suggest therefore neural signatures of error processing in these areas might be specific of cognitive and psychological processes of subjects affected by depression. Similarly, frontal, parietal (including cuneus and precuneus), and temporal areas have been described as altered in studies in late-life MDD (Katz et al., 2010) and in a recent study assessing emotional response inhibition with a Go/No-Go task in MDD and mood disorder subjects (Piani et al., 2022a). These data suggest a wide alteration in attention networks that subside inhibition control in MDD (Cha et al., 2021).

According to our findings, N2 response, which is traditionally associated with conflict monitoring and response inhibition, is accompanied by distinct alterations in the brain's sensory and attentional networks in MDD. Importantly, alterations specific to MDD emerged in the right STG and cerebellum, regions implicated in attentional allocation and cognitive control. The cerebellum's involvement supports its emerging role in managing cognitive processes beyond motor functions, particularly in directing attention during conflict monitoring. Moreover, the altered engagement of the STG aligns with reports of disrupted self-referential processing and emotional regulation in MDD. These results highlight that deficits in MDD extend beyond motor inhibition to include broader disruptions in sensory and attentional mechanisms critical for successful inhibitory control.

4.2. P3 results

In the subsequent stages of stimulus processing, the P3 is thought to be related to processes of response inhibition during "No-Go" trials and response execution during "Go" trials, reflecting conflict resolution and behavior inhibition (Zhang et al., 2023; Monnart et al., 2016).

In our results, target stimuli in "Go/No-Go" blocks (vs. target in "Go" blocks) showed a higher activation of area overlapping with those observed for the N2, such as cerebellar, the SMA, vermis, and precuneus regions in the target "Go/No-Go" (with respect to target "Go") stimuli. Differently from N2, P3 showed higher activation in target "Go/No-Go" (with respect to target "Go" stimuli) in the middle frontal, left precentral, and thalamic regions, regions that were previously reported in previous studies (Swick et al., 2011; Simmonds et al., 2008; Criaud and Boulinguez, 2013; Baumeister et al., 2014). Regarding diagnosis, P3 alterations in MDD are often described during Go/No-Go task and seem to be affected also by age, as shown by Zhang and colleagues (Zhang et al., 2016). In our sample, MDD showed a positive BOLD response in temporal areas, such as the left rolandic operculum, Heschl's gyrus, and parietal areas, including supramarginal gyrus. The supramarginal gyrus is widely known to contribute to phonological word processing and auditory working memory (Sliwinska et al., 2012). Alteration at the level of the supramarginal gyrus might affect impaired response inhibition by the dysfunctional auditory working memory process, thus reflecting a reduced cognitive efficiency for impulse control especially in MDD. A similar result was observed in a recent ERP study conducted on MDD patients (Heo et al., 2022). Additionally, the authors showed that No-Go P3 alterations were led by childhood trauma, a renowned risk factor for psychiatric disorders.

Moreover, parietal connectivity alterations in MDD have been described in both fMRI and EEG studies. A recent EEG study (Chao et al., 2022) suggested that an altered functional connectivity over the parietal–temporal region is associated with rumination, anhedonia and, in general, more severe symptoms in MDD (Mohammadi and Moradi, 2021; Chao et al., 2022). Similarly, a recent rsfMRI study (Wang et al., 2023) showed functional changes in the connectome of MDD patients in temporal and parietal regions, as well as in the bilateral precuneus. Previous studies suggested that frontal regions can modulate high-order cognitive function through connections with lateral parietal cortex (Zhang et al., 2020; Lan et al., 2022) and alterations in these connections in MDD appear to be well documented in Go/No-Go task, including late-life MDD (Zhang et al., 2007). A frontoparietal alteration during cognitive demanding task and response inhibition task could therefore represent a marker of MDD and severity, with possible future clinical application. In this regard, a study showed how frontoparietal activation during response inhibition was able to predict remission with antidepressant treatment, particularly for SSRIs (Gyurak et al., 2016).

Our results suggest that the P3 component, traditionally linked to response inhibition and execution during Go/No-Go tasks, exhibits distinct activation patterns in MDD. The increased activation in temporal regions, such as the left rolandic operculum and Heschl's gyrus, along with the supramarginal gyrus, suggests a disruption in auditory processing and working memory functions. These alterations may contribute to impaired inhibitory control observed in MDD, possibly through dysfunctional auditory working memory processes. Moreover, the involvement of parietal regions is in line with previous studies highlighting their role in cognitive control and their altered connectivity in MDD. These findings indicate the significance of frontoparietal networks in the pathophysiology of MDD, particularly concerning deficits in response inhibition and cognitive control mechanisms.

4.3. Limitations

Multimodal imaging is not without challenges and while it offers many advantages it also requires compromises. The MR environment presents some significant difficulties for recording meaningful EEG. In turn, the magnetic fields of the MRI scanner can be disrupted by the presence of the EEG system inside the scanner. There are artifacts that are specific to the MR environment that need special attention. These artifacts are predominantly due to electromagnetic induction, as described by Faraday's law (Warbrick, 2022). Changes in the magnetic field over time or movement of the components of the EEG system inside the static magnetic field can induce a voltage in the EEG recording circuit. The main artifacts of concern are the gradient artifact, pulse related artifact, and motion related artifact. However, artifacts in our study were addressed in the EEG preprocessing steps, through specific artifact suppression techniques and the use of blind source separation algorithms that had proved effective in our previous works (Maggioni et al., 2014, 2016).

Similarly, some limitations must be considered regarding the sample. The sample size is limited due to the novelty and technicality of the simultaneous EEG and fMRI recording, but in line with similar studies employing the same technique (Fang et al., 2022). Moreover, we tried to balance our sample in terms of age, sex and handedness. MDD patients were medicated, and some medication can alter EEG recording. However, given the heterogeneity of the medication in our dataset, we decided to not include it as covariate for the analysis.

5. Conclusions

This study offered a novel investigation of the neurovascular bases underlying inhibitory control in a group of older adults with late-onset MDD patients, compared to a comparable control group, using a combined EEG-fMRI approach. All participants underwent a visuomotor Go/No-Go task during a simultaneous EEG-fMRI acquisition. Exploiting both techniques' advantages, we provided new insights into altered MDD cognitive processes at different inhibitory control stages,

represented by N2 and P3 ERP peaks. The findings support differences between the hemodynamic correlates of these two peaks especially when investigating the diagnosis effect, highlighting the different processes underlying inhibitory process and its alteration in the MDD patients, especially in sensory processing, attentional control, and cognitive flexibility, highlighting the complexity of the multifactorial MDD.

Declaration of generative AI and AI-assisted technologies in the writing process

During the preparation of this work the authors used ChatGPT in order to improve language and readability. After using this tool/service, the authors reviewed and edited the content as needed and take full responsibility for the content of the publication.

Funding

Paolo Brambilla was partially supported by grants from the Italian Ministry of Education and Research - MUR ('Dipartimenti di Eccellenza' Programme 2023–27 - Dept. of Pathophysiology and Transplantation, Università degli Studi di Milano), the Italian Ministry of Health (Hub Life Science- Diagnostica Avanzata, HLS-DA, PNC-E3-2022-23683266–CUP: C43C22001630001 / MI-0117; Ricerca Corrente 2025; RF-2019-12371349), and by the ERANET Neuron JTC 2023 (ERP-2023-23684211 - ERP-2023-Neuron-ResilNet). Elena Bondi was partially supported by grant from the Italian Ministry of Education and Research - MUR ('Dipartimenti di Eccellenza' Programme 2023–27 - Dept. of Pathophysiology and Transplantation, Università degli Studi di Milano). Eleonora Maggioni was partially supported by the Italian Ministry of University and Research - MUR (PRIN 2022, grant n. 2022RXM3H7) and by the European Union – Next Generation EU (PRIN 2022 PNRR, grant n. P20229MFRC).

Data and code availability statement

The participants of this study did not give written consent for their data to be shared publicly, so due to the sensitive nature of the research supporting data is not available. Data are available for researchers who meet the criteria for access to confidential data through the corresponding author. Matlab codes are available at the Open Science Framework web application link (https://osf.io/uhsb5/?view_only=9848664768564220a9e44af6a831c935).

CRediT authorship contribution statement

Elena Bondi: Writing – review & editing, Writing – original draft, Visualization, Validation, Software, Methodology, Investigation, Formal analysis, Data curation. **Alessandro Pigoni:** Writing – review & editing, Writing – original draft, Validation, Methodology. **Adele Ferro:** Writing – review & editing, Resources. **Maria Pia Marra:** Writing – review & editing, Resources, Investigation. **Guido Nosari:** Writing – review & editing, Resources. **Giandomenico Schiena:** Writing – review & editing, Resources. **Fabio M. Triulzi:** Writing – review & editing, Resources. **Anna M. Bianchi:** Writing – review & editing, Supervision. **Paolo Brambilla:** Writing – review & editing, Supervision, Resources, Project administration, Funding acquisition, Conceptualization. **Eleonora Maggioni:** Writing – review & editing, Writing – original draft, Validation, Supervision, Project administration, Methodology, Funding acquisition, Conceptualization.

Declaration of competing interest

The authors declare the following financial interests/personal relationships which may be considered as potential competing interests:

Elena Bondi reports financial support was provided by Italian Ministry of University and Research. Paolo Brambilla reports was provided by Italian Ministry of University and Research. Eleonora Maggioni reports financial support was provided by Italian Ministry of University and Research. Paolo Brambilla reports financial support was provided by Italian Ministry of Health. Eleonora Maggioni reports financial support was provided by European Union – Next Generation EU. If there are other authors, they declare that they have no known competing financial interests or personal relationships that could have appeared to influence the work reported in this paper.

Supplementary materials

Supplementary material associated with this article can be found, in the online version, at doi:10.1016/j.neuroimage.2025.121320.

Data availability

The participants of this study did not give written consent for their data to be shared publicly, so due to the sensitive nature of the research supporting data is not available. Data are available for researchers who meet the criteria for access to confidential data through the corresponding author.

References

Allen, P.J., Oliver, J., Turner, R., 2000. A method for removing imaging artifact from continuous EEG recorded during functional MRI. Neuroimage 12 (2), 230–239. https://doi.org/10.1006/nimg.2000.0599.

Allen, P.J., Polizzi, G., Krakow, K., Fish, D.R., Lemieux, L., 1998. Identification of EEG events in the MR scanner: the problem of pulse artifact and a method for its subtraction. Neuroimage 8 (3), 229–239. https://doi.org/10.1006/nimg.1998.0361.

Baumeister, S., Hohmann, S., Wolf, I., Plichta, M.M., Rechtsteiner, S., Zangl, M., Ruf, M., et al., 2014. Sequential inhibitory control processes assessed through simultaneous EEG-FMRI. Neuroimage 94, 349–359. https://doi.org/10.1016/j.neuroimage.2014.01.023.

Benikos, N., Johnstone, S.J., Roodenrys, S.J., 2013. Varying task difficulty in the Go/Nogo task: the effects of inhibitory control, arousal, and perceived effort on ERP components. Int. J. Psychophysiol. 87 (3), 262–272. https://doi.org/10.1016/j.ijpsycho.2012.08.005.

Bersani, F.S., Canevelli, M., Cesari, M., Maggioni, E., Pasquini, M., Wolkowitz, O.M., Bruno, G., 2020. Frailty Index as a clinical measure of biological age in psychiatry. J. Affect. Disord. 268, 183–187.

Bessette, K.L., Karstens, A.J., Crane, N.A., Peters, A.T., Stange, J.P., Elverman, K.H., Morimoto, S.S., Weisenbach, S.L., Langenecker, S.A., 2020. A Lifespan model of interference resolution and inhibitory control: risk for depression and changes with illness progression. Neuropsychol. Rev. 30 (4), 477–498. https://doi.org/10.1007/s11065-019-09424-5.

Bokura, H., Yamaguchi, S., Kobayashi, S., 2001. Electrophysiological correlates for response inhibition in a go/NoGo task. Clinic. Neurophysiol. 112 (12), 2224–2232. https://doi.org/10.1016/S1388-2457(01)00691-5.

Bostan, A.C., Dum, R.P., Strick, P.L., 2013. Cerebellar networks with the cerebral cortex and Basal ganglia. Trends Cogn. Sci. (Regul. Ed.) 17 (5), 241–254. https://doi.org/10.1016/j.tics.2013.03.003.

Bullock, M., Jackson, G.D., Abbott, D.F., 2021. Artifact reduction in simultaneous EEG-FMRI: a systematic review of methods and contemporary usage. Front. Neurol. 12 (March). https://doi.org/10.3389/fneur.2021.622719.

Cha, J., Speaker, S., Hu, B., Altinay, M., Koirala, P., Karne, H., Spielberg, J., Kuceyeski, A., Dhamala, E., Anand, A., 2021. Neuroimaging correlates of emotional response-inhibition discriminate between young depressed adults with and without sub-threshold bipolar symptoms (Emotional response-inhibition in young depressed adults). J. Affect. Disord. 281, 303–311. https://doi.org/10.1016/j.jad.2020.12.037.

Chao, Z.C., Daniel, G., Dillon, Y., Liu, H., Barrick, E.M., Wu, C.T., 2022. Altered coordination between frontal delta and parietal alpha networks underlies anhedonia and depressive rumination in major depressive disorder. J. Psychiatry Neurosci. 47 (6), E367–E378. https://doi.org/10.1503/jpn.220046.

Criaud, M., Boulinguez, P., 2013. Have we been asking the right questions when assessing response inhibition in go/No-go tasks with FMRI? A meta-analysis and critical review. Neurosci. Biobehav. Rev. 37 (1), 11–23. https://doi.org/10.1016/j.neubiorev.2012.11.003.

Dai, Q., Feng, Z., 2011. Deficient interference inhibition for negative stimuli in depression: an event-related potential study. Clinic. Neurophysiol. 122 (1), 52–61. https://doi.org/10.1016/j.clinph.2010.05.025.

Debener, S., Ullsperger, M., Siegel, M., Engel, A.K., 2006. Single-trial EEG-FMRI reveals the dynamics of cognitive function. Trends Cogn. Sci. (Regul. Ed.) 10 (12), 558–563. https://doi.org/10.1016/j.tics.2006.09.010.

Debener, S., Ullsperger, M., Siegel, M., Fiehler, K., Yves Von Cramon, D., Engel, A.K., 2005. Trial-by-trial coupling of concurrent electroencephalogram and functional magnetic resonance imaging identifies the dynamics of performance monitoring.

J. Neurosci. 25 (50), 11730–11737. https://doi.org/10.1523/JNEUROSCI.3286-05.2005.
Delorme, A., Makeig, S., 2004. EEGLAB: an open source toolbox for analysis of single-trial EEG dynamics including independent component analysis. J. Neurosci. Methods 134 (1), 9–21. https://doi.org/10.1016/j.jneumeth.2003.10.009.
Donkers, FC.L., Boxtel, G.J.M.V., 2004. The N2 in go/No-go tasks reflects conflict monitoring not response inhibition. Brain Cogn. 56 (2 SPEC. ISS), 165–176. https://doi.org/10.1016/j.bandc.2004.04.005.
Dotson, V.M., McClintock, S.M., Verhaeghen, P., Kim, J.U., Draheim, A.A., Syzmkowicz, S.M., Gradone, A.M., Bogoian, H.R., Wit, L.D., 2020. Depression and cognitive control across the lifespan: a systematic review and meta-analysis. Neuropsychol. Rev. 30 (4), 461–476. https://doi.org/10.1007/s11065-020-09436-6.
Eimer, M., 1993. Effects of attention and stimulus probability on ERPs in a Go/Nogo task. Biol. Psychol. 35 (2), 123–138. https://doi.org/10.1016/0301-0511(93)90009-W.
Elm, E., Altman, D.G., Egger, M., Pocock, S.J., Gøtzsche, P.C., Vandenbroucke, J.P., 2014. The strengthening the reporting of observational studies in epidemiology (STROBE) statement: guidelines for reporting observational studies. Int. J. Surg. 12 (12). https://doi.org/10.1016/j.ijsu.2014.07.013.
Enriquez-Geppert, S., Konrad, C., Pantev, C., Huster, R.J., 2010. Conflict and inhibition differentially affect the N200/P300 complex in a combined go/nogo and stop-signal task. Neuroimage 51 (2), 877–887. https://doi.org/10.1016/j.neuroimage.2010.02.043.
Falkenstein, M., Hoormann, J., Hohnsbein, J., 1999. ERP components in Go/Nogo tasks and their relation to inhibition. Acta Psychol. 101 (2–3), 267–291. https://doi.org/10.1016/s0001-6918(99)00008-6.
Fang, Z., Lynn, E., Huc, M., Fogel, S., Knott, V.J., Jaworska, N., 2022. Simultaneous EEG + FMRI study of brain activity during an emotional stroop task in individuals in remission from depression. Cortex 155, 237–250. https://doi.org/10.1016/j.cortex.2022.07.010.
Garavan, H., Ross, T.J., Stein, E.A., 1999. Right hemispheric dominance of inhibitory control: an event-related functional MRI study. Proc. Natl. Acad. Sci. U.S.A. 96 (14), 8301–8306. https://doi.org/10.1073/pnas.96.14.8301.
Gyurak, A., Patenaude, B., Korgaonkar, M.S., Grieve, S.M., Williams, L.M., Etkin, A., 2016. Frontoparietal activation during response inhibition predicts remission to antidepressants in patients with major depression. Biol. Psychiatry 79 (4), 274–281. https://doi.org/10.1016/j.biopsych.2015.02.037.
Hamilton, M., 1960. A rating scale for depression. J. Neurol. Neurosurg. Psychiatry 23 (1), 56–62. https://doi.org/10.1136/jnnp.23.1.56.
Han, Y.L., Dai, Z.P., Ridwan, M.C., Lin, P.H., Zhou, H.L., Wang, H.F., Yao, Z.J., Lu, Q., 2020. Connectivity of the frontal cortical oscillatory dynamics underlying inhibitory control during a go/No-go task as a predictive biomarker in major depression. Front. Psychiatry 11 (August). https://doi.org/10.3389/fpsyt.2020.00707.
Heo, I.S., Kwon, Y.J., Lee, H.Y., Lee, H.S., Yoon, H.J., Shim, S.H., Kim, J.S., 2022. Electrophysiological changes related to childhood trauma in patients with major depressive disorder: an event-related potential study. Clinic. Psychopharmacol. Neurosci. 20 (1), 167–179. https://doi.org/10.9758/CPN.2022.20.1.167.
Huster, R.J., Westerhausen, R., Pantev, C., Konrad, C., 2010. The role of the cingulate cortex as neural generator of the N200 and P300 in a tactile response inhibition task. Hum. Brain Mapp. 31 (8), 1260–1271. https://doi.org/10.1002/hbm.20933.
Iannaccone, R., Hauser, T.U., Staempfli, P., Walitza, S., Brandeis, D., Brem, S., 2015. Conflict monitoring and error processing: new insights from simultaneous EEG-FMRI. Neuroimage 105, 395–407. https://doi.org/10.1016/j.neuroimage.2014.10.028.
Jenkinson, M., Beckmann, C.F., Behrens, T.E.J., Woolrich, M.W., Smith, S.M., 2012. FSL. Neuroimage 62 (2), 782–790. https://doi.org/10.1016/J.NEUROIMAGE.2011.09.015.
Jia, H., Li, H., Yu, D., 2017. The relationship between ERP components and EEG spatial complexity in a visual go/nogo task. J. Neurophysiol. 117 (1), 275–283. https://doi.org/10.1152/jn.00363.2016.
Joormann, J., Yoon, K.L., Zetsche, U., 2007. Cognitive inhibition in depression. Appl. Prevent. Psychol. 12 (3), 128–139. https://doi.org/10.1016/j.appsy.2007.09.002.
Jorge, J., Van der Zwaag, W., Figueiredo, P., 2014. EEG-FMRI integration for the study of Human brain function. Neuroimage 102 (P1), 24–34. https://doi.org/10.1016/j.neuroimage.2013.05.114.
Kaiser, S., Unger, J., Kiefer, M., Markela, J., Mundt, C., Weisbrod, M., 2003. Executive control deficit in depression: event-related potentials in a Go/Nogo task. Psychiatry Res. Neuroimaging 122 (3), 169–184. https://doi.org/10.1016/S0925-4927(03)00004-0.
Kandilarova, S., Stoyanov, D., Sirakov, N., Maes, M., Specht, K., 2019. Reduced grey matter volume in frontal and temporal areas in depression: contributions from voxel-based morphometry study. Acta Neuropsychiatr. 31 (5), 252–257. https://doi.org/10.1017/neu.2019.20.
Karch, S., Voelker, J.M., Thalmeier, T., Ertl, M., Leicht, G., Pogarell, O., Mulert, C., 2014. Deficits during voluntary selection in adult patients with ADHD: new insights from single-trial coupling of simultaneous EEG/FMRI. Front. Psychiatry 5 (APR). https://doi.org/10.3389/fpsyt.2014.00041.
Katz, R., De Sanctis, P., Mahoney, J.R., Sehatpour, P., Murphy, C.F., Gomez-Ramirez, M., Alexopoulos, G.S., Foxe, J.J., 2010. Cognitive control in late-life depression: response inhibition deficits and dysfunction of the anterior cingulate cortex. Am. J. Geriatr. Psychiatry 18 (11), 1017–1025. https://doi.org/10.1097/JGP.0b013e3181d695f2.
Knyazev, G.G., Savostyanov, A.N., Bocharov, A.V., Brak, I.V., Osipov, E.A., Filimonova, E.A., Saprigyn, A.E., Aftanas, L.I., 2018. Task-positive and task-negative networks in major depressive disorder: a combined FMRI and EEG study. J. Affect. Disord. 235, 211–219. https://doi.org/10.1016/j.jad.2018.04.003.
Lan, Z., Zhang, W., Wang, D., Tan, Z., Wang, Y., Pan, C., Xiao, Y., Kuai, C., Xue, S.W., 2022. Decreased modular segregation of the frontal–Parietal network in major depressive disorder. Front. Psychiatry 13 (July). https://doi.org/10.3389/fpsyt.2022.929812.
Li, N., Di, J., Wei, J., Huang, Y., Xu, J., 2022. Functional brain abnormalities in major depressive disorder using a multiscale community detection approach. Neuroscience 501 (October), 1–10. https://doi.org/10.1016/j.neuroscience.2022.08.007.
Maggioni, E., Arrubla, J., Warbrick, T., Dammers, J., Bianchi, A.M., Reni, G., Tosetti, M., Neuner, I., Jon Shah, N., 2014. Removal of pulse artefact from EEG data recorded in MR environment at 3T setting of ICA parameters for marking artefactual components: application to resting-state data. PLoS One 9 (11). https://doi.org/10.1371/journal.pone.0112147.
Maggioni, E., Zucca, C., Reni, G., Cerutti, S., Triulzi, F.M., Bianchi, A.M., Arrigoni, F., 2016. Investigation of the electrophysiological correlates of negative BOLD response during intermittent photic stimulation: an EEG-FMRI study. Hum. Brain Mapp. 37 (6), 2247–2262. https://doi.org/10.1002/hbm.23170.
Malejko, K., Hafner, S., Plener, P.L., Bonenberger, M., Groen, G., Abler, B., Graf, H., 2021. Neural signature of error processing in major depression. Eur. Arch. Psychiatry Clin. Neurosci. 271 (7), 1359–1368. https://doi.org/10.1007/s00406-021-01238-y.
Mannarelli, D., Pauletti, C., Petritis, A., Delle Chiaie, R., Currà, A., Trompetto, C., Fattapposta, F., 2020. Effects of cerebellar TDCS on inhibitory control: evidence from a go/NoGo task. Cerebellum. 19 (6), 788–798. https://doi.org/10.1007/s12311-020-01165-z.
Mayeli, A., Zotev, V., Refai, H., Bodurka, J., 2016. Real-time EEG artifact correction during FMRI using ICA. J. Neurosci. Methods 274, 27–37. https://doi.org/10.1016/j.jneumeth.2016.09.012.
Mayhew, S.D., Ostwald, D., Porcaro, C., Bagshaw, A.P., 2013. Spontaneous EEG alpha oscillation interacts with positive and negative BOLD responses in the visual-auditory cortices and default-mode network. Neuroimage 76 (August), 362–372. https://doi.org/10.1016/j.neuroimage.2013.02.070.
McMillan, R., Sumner, R., Forsyth, A., Campbell, D., Malpas, G., Maxwell, E., Deng, C., et al., 2020. Simultaneous EEG/FMRI recorded during ketamine infusion in patients with major depressive disorder. Prog. Neuro-Psychopharmacol. Biol. Psychiatry 99. https://doi.org/10.1016/j.pnpbp.2019.109838.
Miyake, A., Emerson, M.J., Friedman, N.P., 2000. Assessment of executive functions in clinical settings: problems and recommendations. Semin. Speech. Lang. 21 (2), 169–183. https://doi.org/10.1055/s-2000-7563.
Mohammadi, Y., Moradi, M.H., 2021. Prediction of depression severity scores based on functional connectivity and complexity of the EEG signal. Clin. EEG Neurosci. 52 (1), 52–60. https://doi.org/10.1177/1550059420965431.
Monnart, A., Kornreich, C., Verbanck, P., Campanella, S., 2016. Just swap out of negative vibes? Rumination and inhibition deficits in major depressive disorder: data from event-related potentials studies. Front. Psychol. 7 (JUL), 190730. https://doi.org/10.3389/fpsyg.2016.01019.
Mulert, C., Seifert, C., Leicht, G., Kirsch, V., Ertl, M., Karch, S., Moosmann, M., et al., 2008. Single-trial coupling of EEG and FMRI reveals the involvement of early anterior cingulate cortex activation in effortful decision making. Neuroimage 42 (1), 158–168. https://doi.org/10.1016/j.neuroimage.2008.04.236.
Murphy, F.C., Sahakian, B..J., Rubinsztein, J.S., Michael, A., Rogers, R.D., Robbins, T.W., Paykel, E.S., 1999. Emotional bias and inhibitory control processes in mania and depression. Psychol. Med. 29 (6), 1307–1321. https://doi.org/10.1017/S0033291799001233.
Narumoto, J., Okada, T., Sadato, N., Fukui, K., Yonekura, Y., 2001. Attention to emotion modulates FMRI activity in Human right superior temporal sulcus. Cogn. Brain Res. 12 (2), 225–231. https://doi.org/10.1016/S0926-6410(01)00053-2.
Nieuwenhuis, S., Yeung, N., Wildenberg, W.V.D., Richard Ridderinkhof, K., 2003. Electrophysiological correlates of anterior cingulate function in a go/No-go task: effects of response conflict and trial type frequency. Cogn. Affect. Behav. Neurosci. 3 (1), 17–26. https://doi.org/10.3758/CABN.3.1.17.
Norman, D.A., and T. Shallice. 1986. “Attention to action.” *Consciousness and Self-Regulation*, 1–18. 10.1007/978-1-4757-0629-1_1.
Penny, W., K. Friston, J. Ashburner, S. Kiebel, and T. Nichols. 2007. “Statistical parametric mapping: the analysis of functional brain images.” Statistical Parametric Mapping: The Analysis of Functional Brain Images. 2007. 10.1016/B978-0-12-372560-8.X5000-1.
Pfefferbaum, A., Ford, J.M., Weller, B.J., Kopell, B.S., 1985. ERPs to response production and inhibition. Electroencephalogr. Clin. Neurophysiol. 60 (5), 423–434. https://doi.org/10.1016/0013-4694(85)91017-X.
Piani, M.C., Maggioni, E., Delvecchio, G., Brambilla, P., 2022a. Sustained attention alterations in major depressive disorder: a review of FMRI studies employing go/No-go and CPT tasks. J. Affect. Disord. 303, 98–113. https://doi.org/10.1016/j.jad.2022.02.003.
Piani, M.C., Maggioni, E., Delvecchio, G., Ferro, A., Gritti, D., Pozzoli, S.M., Fontana, E., et al., 2022b. Sexual dimorphism in the brain correlates of adult-onset depression: a pilot structural and functional 3T MRI study. Front. Psychiatry 12 (January), 683912. https://doi.org/10.3389/fpsyt.2021.683912.
Pigoni, A., Tesic, I., Pini, C., Enrico, P., Di Consoli, L., Siri, F., Nosari, G., et al., 2025. Multimodal machine learning prediction of 12-month suicide attempts in bipolar disorder. Bipolar. Disord. 0 (March), 1–15. https://doi.org/10.1111/BDI.70011.
Polich, J., 2007. Updating P300: an integrative theory of P3a and P3b. Clin. Neurophysiol. 118 (10), 2128–2148. https://doi.org/10.1016/j.clinph.2007.04.019.
Quinn, C.R., Harris, A., Kemp, A.H., 2012. The impact of depression heterogeneity on inhibitory control. Aust. N. Z. J. Psychiatry 46 (4), 374–383. https://doi.org/10.1177/0004867411432073.
Randolph, C., Tierney, M.C., Mohr, E., Chase, T.N., 1998. The Repeatable Battery for the Assessment of Neuropsychological Status (RBANS): Preliminary clinical validity.

J. Clin. Exp. Neuropsycho. 20 (3), 310–319. https://doi.org/10.1076/jcen.20.3.310.823.
Reed, C.L., Leland, D.S., Brekke, B., Hartley, A.A., 2013. Attention's grasp: early and late hand proximity effects on visual evoked potentials. Front. Psychol. 4 (JUL). https://doi.org/10.3389/fpsyg.2013.00420.
Rentrop, M., Backenstrass, M., Jaentsch, B., Kaiser, S., Roth, A., Unger, J., Weisbrod, M., Renneberg, B., 2007. Response inhibition in Borderline Personality Disorder: performance in a Go/Nogo task. Psychopathology 41 (1), 50–57. https://doi.org/10.1159/000110626.
Richard-Devantoy, S., Ding, Y., Lepage, M., Turecki, G., Jollant, F., 2016. Cognitive inhibition in depression and suicidal behavior: a neuroimaging study. Psychol. Med. 46 (5), 933–944. https://doi.org/10.1017/S0033291715002421.
Rolls, E.T., Huang, C.C., Lin, C.P., Feng, J., Joliot, M., 2020. Automated anatomical labelling atlas 3. Neuroimage 206. https://doi.org/10.1016/j.neuroimage.2019.116189.
Ruchsow, M., Groen, G., Kiefer, M., Beschoner, P., Hermle, L., Ebert, D., Falkenstein, M., 2008. Electrophysiological evidence for reduced inhibitory control in depressed patients in partial remission: a Go/Nogo study. Int. J. Psychophysiol. 68 (3), 209–218. https://doi.org/10.1016/j.ijpsycho.2008.01.010.
Shaffer, J.J., Willour, V., Fiedorowicz, J.G., Christensen, G.E., Long, J.D., Johnson, C.P., Schmitz, S.L., Williams, A.J., Wemmie, J., Magnotta, V.A., 2022. Distinct patterns of altered quantitative T1ρ and functional BOLD response associated with history of suicide attempts in bipolar disorder. Brain Imaging Behav. 1–14. https://doi.org/10.1007/s11682-021-00552-2.
Simmonds, D.J., Pekar, J.J., Mostofsky, S.H., 2008. Meta-analysis of go/No-go tasks demonstrating that FMRI activation associated with response inhibition is task-dependent. Neuropsychologia 46 (1), 224–232. https://doi.org/10.1016/j.neuropsychologia.2007.07.015.
Sliwinska, M.W., Khadilkar, M., Campbell-Ratcliffe, J., Quevenco, F., Devlin, J.T., 2012. Early and sustained supramarginal gyrus contributions to phonological processing. Front. Psychol. 3 (MAY). https://doi.org/10.3389/fpsyg.2012.00161.
Swick, D., Ashley, V., Turken, U., 2011. Are the neural correlates of stopping and not going identical? Quantitative meta-analysis of two response inhibition tasks. Neuroimage 56 (3), 1655–1665. https://doi.org/10.1016/j.neuroimage.2011.02.070.
Takahashi, T., Yücel, M., Lorenzetti, V., Walterfang, M., Kawasaki, Y., Whittle, S., Suzuki, M., Pantelis, C., Allen, N.B., 2010. An MRI study of the superior temporal subregions in patients with current and past major depression. Prog. Neuro-Psychopharmacol. Biol. Psychiatry 34 (1), 98–103. https://doi.org/10.1016/j.pnpbp.2009.10.005.
Tikàsz, A., Potvin, S., Richard-Devantoy, S., Lipp, O., Hodgins, S., Lalonde, P., Lungu, O., Dumais, A., 2018. Reduced dorsolateral prefrontal cortex activation during affective go/NoGo in violent schizophrenia patients: an FMRI study. Schizophr. Res. 197, 249–252. https://doi.org/10.1016/j.schres.2017.11.011.
Tozzi, L., Goldstein-Piekarski, A.N., Korgaonkar, M.S., Williams, L.M., 2020. Connectivity of the cognitive Control network during response inhibition as a predictive and response biomarker in major depression: evidence from a randomized clinical trial. Biol. Psychiatry 87 (5), 462–472. https://doi.org/10.1016/j.biopsych.2019.08.005.
Tymofiyeva, O., Reeves, K.W., Shaw, C., Lopez, E., Aziz, S., Max, J.E., Yang, T.T., 2023. A systematic review of MRI studies and the 'emotional PaiN and social disconnect (END)' brain model of suicidal behavior in youth. Behav. Neurol. 2023 (1), 7254574. https://doi.org/10.1155/2023/7254574.
Vallesi, A., 2011. Targets and non-targets in the aging brain: a go/Nogo event-related potential study. Neurosci. Lett. 487 (3), 313–317. https://doi.org/10.1016/j.neulet.2010.10.046.
Wang, L., Ma, Q., Sun, X., Xu, Z., Zhang, J., Liao, X., Wang, X., et al., 2023. Frequency-resolved connectome alterations in major depressive disorder: a multisite resting FMRI study. J. Affect. Disord. 328, 47–57. https://doi.org/10.1016/j.jad.2023.01.104.
Warbrick, T., 2022. Simultaneous EEG-FMRI: what have we learned and what does the future hold? Sensors 22 (6). https://doi.org/10.3390/s22062262.
Wauthia, E., Rossignol, M., 2016. Emotional processing and attention control impairments in children with anxiety: an integrative review of event-related potentials findings. Front. Psychol. 7 (MAY). https://doi.org/10.3389/fpsyg.2016.00562.
Wessa, M., Houenou, J., Paillère-Martinot, M.L., Berthoz, S., Artiges, E., Leboyer, M., Martinot, J.L., 2007. Fronto-striatal overactivation in euthymic bipolar patients during an emotional Go/Nogo task. Am. J. Psychiatry 164 (4), 638–646. https://doi.org/10.1176/ajp.2007.164.4.638.
Zhang, B.W., Xu, J., Chang, Y., 2016. The effect of aging in inhibitory control of major depressive disorder revealed by event-related potentials. Front. Hum. Neurosci. 10 (MAR2016), 1–10. https://doi.org/10.3389/fnhum.2016.00116.
Zhang, B.W., Zhao, L., Xu, J., 2007. Electrophysiological activity underlying inhibitory control processes in late-life depression: a Go/Nogo study. Neurosci. Lett. 419 (3), 225–230. https://doi.org/10.1016/j.neulet.2007.04.013.
Zhang, H., Palaniyappan, L., Wu, Y., Cong, E., Wu, C., Ding, L., Jin, F., et al., 2020. The concurrent disturbance of dynamic functional and structural brain connectome in major depressive disorder: the prefronto-insular pathway. J. Affect. Disord. 274, 1084–1090. https://doi.org/10.1016/j.jad.2020.05.148.
Zhang, X., Jia, H., Wang, E., 2023. Negative inhibition is poor in sub-threshold depression individuals: evidence from ERP and a go/No-go task. Psychiatry Res. - Neuroimaging 331, 111638. https://doi.org/10.1016/j.pscychresns.2023.111638.
Zhao, P., Wang, X., Wang, Q., Yan, R., Ridwan Chattun, M., Yao, Z., Lu, Q., 2023. Altered fractional amplitude of low-frequency fluctuations in the superior temporal gyrus: a resting-state FMRI study in anxious depression. BMC Psychiatry 23 (1). https://doi.org/10.1186/s12888-023-05364-w.